

Paramyotonia Congenita: The R1448P Na⁺ Channel Mutation in Adult Human Skeletal Muscle

H. Lerche, MD,*‡ N. Mitrovic, MD,*‡ V. Dubowitz, MD,† and F. Lehmann-Horn, MD*

Twitch force and Na⁺ currents were investigated in a muscle biopsy specimen from a patient with paramyotonia congenita carrying the dominant Arg-1448-Pro mutation in the skeletal muscle sodium channel. Cooling of the muscle fibers caused sustained membrane depolarization that resulted in reduced twitch force. Membrane repolarization, produced by a K⁺ channel opener, partly prevented and antagonized the drop in twitch force. Patch-clamp recordings on sarcolemmal blebs revealed a distinctly slower Na⁺ current decay on paramyotonia congenita muscle compared to control muscle. In addition, patches with mutant Na⁺ channels showed a significantly higher frequency of steady-state openings, which increased with cooling. Activation of mutant channels was not affected, whereas the steady-state inactivation curve was shifted by -5 mV and showed less voltage dependence. We suggest that the weakness of cooled muscle can be explained by a combination of the increased steady-state Na⁺ current and the left-shifted inactivation curve.

Lerche H, Mitrovic N, Dubowitz V, Lehmann-Horn F. Paramyotonia congenita: the R1448P Na⁺ channel mutation in adult human skeletal muscle. *Ann Neurol* 1996;39:599-608

Three autosomal dominant muscle diseases—hyperkalemic periodic paralysis (HyperPP), paramyotonia congenita (PC), and potassium-aggravated myotonia (PAM)—are caused by point mutations in the α -subunit of the adult skeletal muscle Na⁺ channel. To date, 16 mutations that cause these so-called Na⁺ channelopathies have been detected [1]. The hallmarks of PC are paradoxical myotonia, that is, muscle stiffness that becomes more severe with exercise, and weakness triggered by exposure to cold, whereas temperature dependence is not a typical sign of PAM and HyperPP. HyperPP is characterized by episodic weakness, sometimes accompanied by myotonia, and PAM by muscle stiffness aggravated by oral potassium loading, typically without weakness.

Prior to genetic studies, voltage-clamp experiments on native or cultured samples of muscle biopsy specimens from patients revealed incomplete inactivation of the sodium channels to be a major defect in Na⁺ channelopathies [2-6]. Studies of heterologously expressed mutant Na⁺ channels confirmed this result and provided more details as to the malfunction of the Na⁺ channels, such as a shift in gating modes, accelerated recovery from inactivation, increased "window current," and uncoupling of activation from inactivation [7-12].

Studies of native tissue have become rare since heterologous expression systems have taken over. With these systems, there is no shortage of tissue to be examined and, moreover, the differences between mutant and wild-type channels become more obvious because the channel populations are homogeneous. However, channel gating may depend on the system [13], and it is not known to what extent the effects of the mutations measured in cell lines can be extrapolated to muscle fibers. For instance, the expression rate could be influenced by the mutation. A value of 50% mutant channels is predicted by the dominant mode of inheritance of the Na⁺ channel diseases; however, the *in vivo* percentage is not known. Thus, it seems important to continue studies on preparations obtained from patients. Moreover, these studies enable correlation of patch-clamp results with other muscle fiber parameters such as force development or resting potentials.

In this study, we performed a muscle biopsy to examine the functional consequences of the Arg-1448-Pro Na⁺ channel mutation. This mutation causes a clinically severe form of PC, including paradoxical myotonia in a warm environment, cold-induced muscle stiffness followed by weakness, and toe walking due to muscle shortening [14].

From the *Department of Applied Physiology, University of Ulm, Ulm, Germany, and the †Department of Pediatrics and Neonatal Medicine, Hammersmith Hospital, London, United Kingdom.

‡Drs Lerche and Mitrovic contributed equally to this study.

Received Sep 5, 1995, and in revised form Nov 27. Accepted for publication Nov 29, 1995.

Address correspondence to Dr Lehmann-Horn, Department of Applied Physiology, University of Ulm, D-89069 Ulm, Germany.

Materials and Methods

Muscle Preparation

The patient (and her parents) gave informed consent to a quadriceps muscle biopsy. Control muscle specimens were obtained from individuals who had undergone muscle biopsy for exclusion of malignant hyperthermia susceptibility. The specimens removed under local or regional anesthesia were about 3 cm in length and 0.5 cm in diameter. They were then divided into bundles of about 2 mm in diameter. All procedures were in accordance with the Helsinki convention and were approved by the Ethical Committee of the University of Ulm.

Force and Conventional Voltage-Clamp

Measurements

Isometric contractions were induced by supramaximal field stimulation at a frequency of 0.1 Hz and recorded using a force transducer. The temperature was controlled via a water bath and continuously measured within the recording chamber. To determine the steady-state relationship between membrane current density and membrane potential, resealed fiber segments [15] were impaled midway between the ends with three capacity-compensated microelectrodes. The voltage-clamp setup and the experimental protocol used have been described elsewhere [16].

The standard solution used for *in vitro* force and three microelectrode voltage-clamp measurements contained (in mmol/liter) sodium chloride (NaCl), 108; potassium chloride (KCl), 3.5; calcium chloride (CaCl₂), 1.5; magnesium sulfate (MgSO₄), 0.7; sodium bicarbonate (NaHCO₃), 26.2; NaH₂PO₄, 1.7; sodium gluconate, 9.6; glucose, 5.5; sucrose, 7.6; and 315 mOsm/liter (pH 7.4), kept at 37°C. For transportation and dissection, 1 μmol of tetrodotoxin (TTX) (Roth, Karlsruhe, Germany) per liter was added to ensure stable resting potentials since it was known from earlier studies that PC muscle fibers otherwise depolarize and hardly recover. TTX was washed out over several hours prior to the experiments. Some solutions contained the K⁺ channel opener bimakalim (EMD52692, Merck, Darmstadt, Germany).

Patch Clamp

Standard single-channel recording [17] was performed on mechanically prepared sarcolemmal blebs [18]. The solution used for transportation and dissection contained (in mmol/liter) potassium methanesulfonate, 130; magnesium chloride (MgCl₂), 2; ethyleneglycoltetraacetic acid (EGTA), 2; and HEPES, 5 (pH 7.2). All currents were recorded from bleb-attached patches (for details see [6, 19]). In macropatches (Na⁺ currents ranging from 30–300 pA), leakage and capacitive currents were automatically subtracted by means of a prepulse protocol ($-P/4$) and Na⁺ currents were averaged 5 to 15 times. Currents were filtered at 3 kHz and digitized at a 20-kHz sampling rate using pClamp 6.0.1 (Axon Instruments, Foster City, CA). Leakage and capacitive currents were eliminated by subtracting averaged and scaled records without channel activity when late Na⁺ currents, first latencies, and mean open time distributions were analyzed. The number of channels present in the patch was estimated by inspecting traces and counting the maximum number of

channels that open simultaneously [20]. Single-channel recordings were filtered at 2 kHz and sampled at 20 kHz. The data were analyzed by a combination of pClamp, homemade, and SigmaPlot software (Jandel Scientific, San Rafael, CA).

The pipette solution contained (in mmol/liter) NaCl, 130; KCl, 4; MgCl₂, 1; CaCl₂, 2; and HEPES, 10 (pH 7.4); the bathing solution contained CsCl, 130; NaCl, 5; CaCl₂, 1; MgCl₂, 2; and HEPES, 10 (pH 7.2). As previously shown, the bathing solution entered the sarcolemmal blebs during their formation, so that it was present at the intracellular side of the patch-clamped cell membrane. Therefore, bleb resting potentials were assumed to be zero [6, 19].

For statistical evaluation, Student's *t* test was applied. All data are shown as means ± standard error of mean.

Results

Patient History

The patient's history and clinical examination have been provided elsewhere [14]. This 10-year-old girl, living with a foster mother since the age of 3, had had symptoms of paramyotonia since early childhood. When playing outdoors, her eyes got small and her fingers stiffened. A cold bath induced stiffness and there was one episode when she was unable to walk or even move for 1 to 2 hours after swimming. Her gait was never normal. In particular in the morning she walked on her toes and complained about pain in her calves. She had never had an episode of complete flaccid paralysis occurring spontaneously in a warm environment.

On examination she showed muscle stiffness increasing with repetitive tight closures of her eyes and to a lesser degree, after clenching her fist for several times (paradoxical myotonia). When her hand was immersed in 16°C cold water, a bizarre, stiff position developed. Needle electromyography (EMG) taken from the right flexor digitorum muscle at this time showed fibrillation-like spontaneous spiking and some myotonic discharges (a typical finding in a cooled paramyotonic muscle). It took about 1 hour for the hand to return to normal.

Histology revealed a somewhat hypertrophic muscle tissue with very slight unspecific myopathic changes (e.g., borderline number of central nuclei and variation in fiber size). According to histochemical criteria, a lack of type IIb fibers is possible. No inflammatory signs were observed. Electron microscopic analysis did not reveal pathological alterations. These results are compatible with the diagnosis of PC.

In Vitro Force Measurements

At 37°C, the patient's muscle bundles contracted with a constant isometric force. Cooling induced an immediate loss of force to less than 20% of its initial value, and on rewarming, muscle force only recovered slowly

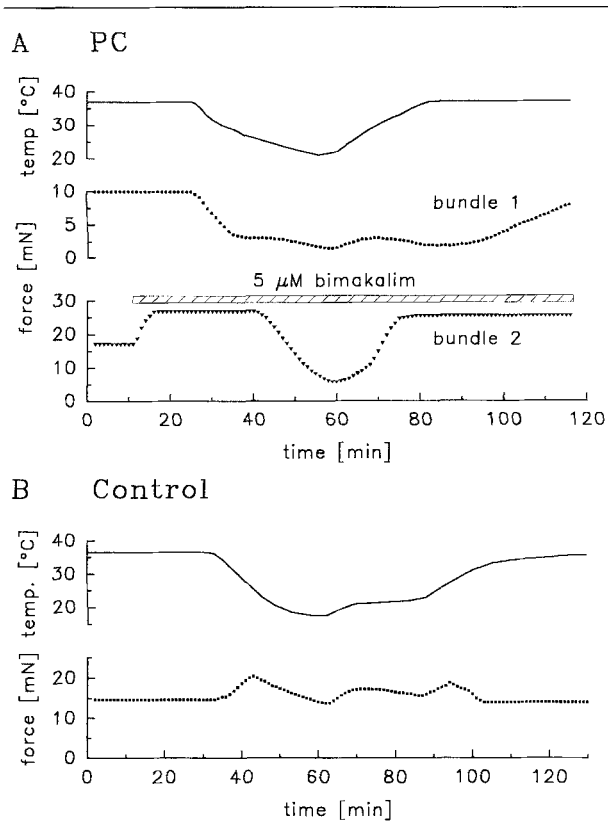


Fig 1. Cold-induced weakness *in vitro*. (A) Force development on cooling and rewarming of two biopsied muscle bundles from the paramyotonia congenita (PC) patient; bundle 2 was treated with the potassium channel opener bimakalim for the indicated period (lower panel). The upper panel shows continuous recording of the temperature. (B) Same procedure as in (A) for a muscle bundle from a normal control person. Single twitches were induced at a frequency of 0.1 Hz; each data point is the average of six twitches.

(Fig 1A, bundle 1). Assuming that the paralysis was due to sustained and marked membrane depolarization, we exposed a second bundle (simultaneously to bundle 1) to a K⁺ channel opener (bimakalim) known to hyperpolarize the cell membrane by opening ATP-dependent K⁺ channels [18, 21, 22]. Indeed, bimakalim (5 μmol/liter) prevented weakness as long as the bath temperature did not fall below 26°C, a temperature at which bundle 1 had already lost 75% of its force. Further cooling induced paralysis to a similar extent as observed without bimakalim; however, recovery from paralysis occurred much faster and the force reached almost its initial value at 26°C (Fig 1A, bundle 2). This experiment was reproduced with two more muscle bundles from the patient. In another bundle, bimakalim (10 μmol/liter) was able to antagonize the weakness occurring at a constant temperature of 23°C (not shown). In control muscle, cooling and rewarming induced some transient changes in twitch force, but significant muscle weakness did not occur (Fig 1B).

Thus, a certain threshold potential at which the membrane becomes inexcitable and the muscle paralyzed must have been exceeded. In the presence of bimakalim, paralysis occurred presumably when the depolarizing effect of noninactivating Na⁺ channels overcame the hyperpolarizing action of the K⁺ channel opener.

Intracellular Microelectrode Measurements

Resealed muscle fiber segments had normal resting membrane potentials of -80.0 ± 0.4 mV ($n = 5$) in standard solution containing 1 μmol of TTX per liter at 37°C. When TTX was washed out, many fibers, but not all, depolarized to values between -60 and -65 mV. Cooling to 25°C caused further depolarization to -44.4 ± 0.8 mV ($n = 19$). After rewarming, the fibers partially recovered within about half an hour and showed potentials of -60.1 ± 1.0 mV ($n = 9$). Spontaneous activity was not observed.

The steady-state current-voltage relationship was determined by use of three microelectrodes in TTX-free standard solution. The slope of this relationship reflects the total membrane conductance, which yielded 190 ± 3 S/cm² (6) at 37°C and 292 ± 5 S/cm² (6) at 25°C (both values were determined at the holding potential of -80 mV). The relationship recorded at 37°C slightly resembled a so-called N shape, probably due to a small steady-state inward current conducted during depolarization steps. The larger slope conductance at a low temperature is consistent with a further increase of the inward current at -80 mV, as has already been described in detail in earlier studies on PC patients [3, 16].

Patch-Clamp Recordings

Na⁺ currents on sarcolemmal blebs of native muscle specimens from control subjects and from the patient carrying the R1448P mutation were analyzed using macropatches and single-channel recordings (see Materials and Methods).

ANALYSIS OF MACROPATCHES. Families of Na⁺ currents were elicited by various depolarizing steps from a prepulse potential of -140 mV (holding potential -100 mV). The most significant result was that "paramyotonic" currents decayed more slowly than those from controls (Fig 2A). Normalized I-V plots were almost identical for PC and control patches (Fig 2B). The corresponding conductance-voltage plots (not shown) were fitted with the standard Boltzmann equation $I/I_{\max} = (1 + \exp[(V - V_{0.5})/k_V])^{-1}$, in which $V_{0.5}$ is the potential of half-maximal activation and k_V the slope factor. $V_{0.5}$ and k_V were -32.0 ± 1.0 mV and -9.6 ± 0.1 mV ($n = 12$) for control patches, and 30.5 ± 1.8 mV and -9.8 ± 0.2 mV ($n = 7$) for PC patches.

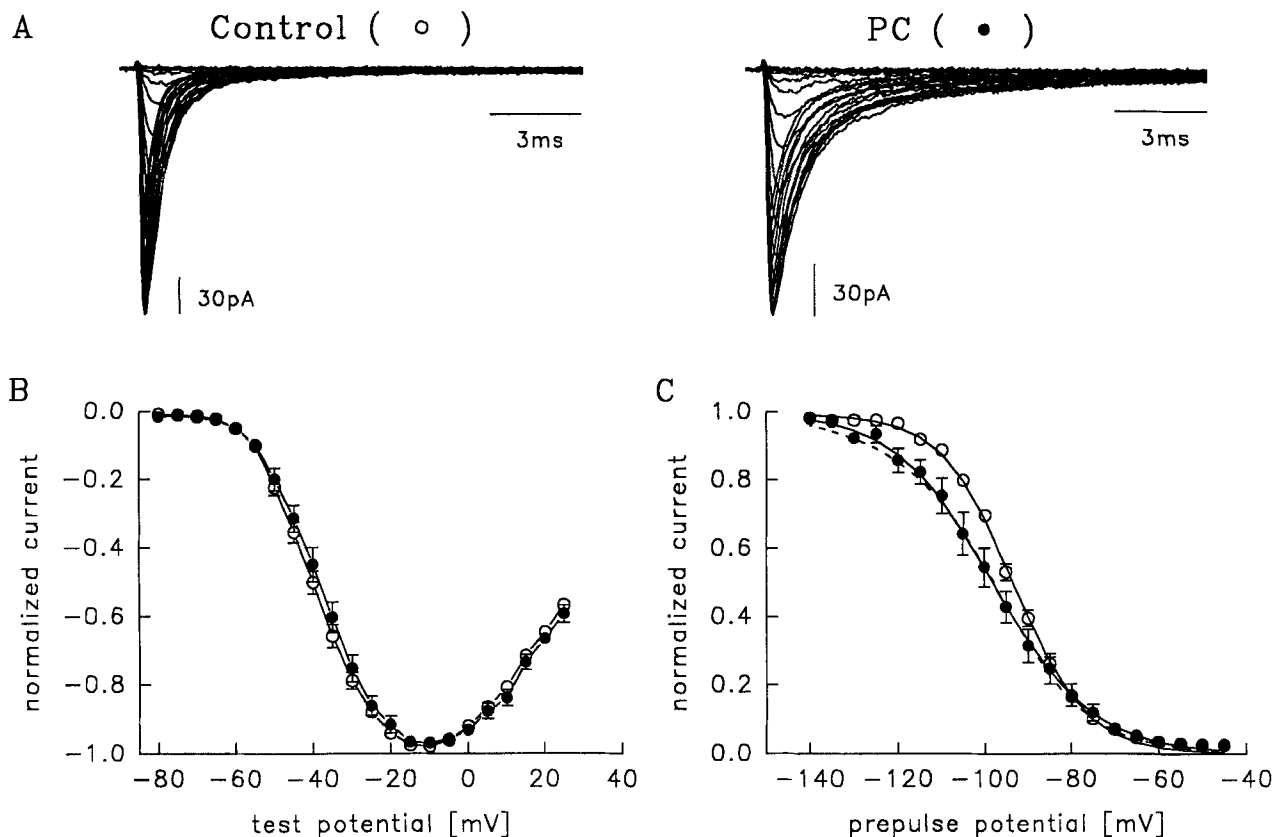


Fig 2. Sodium currents in macropatches. (A) Family of sodium currents elicited by depolarizing test pulses (potentials indicated in B) from a prepulse potential of -140 mV (holding -100 mV) for control and paramyotonia congenita (PC) patches. (B) Current-voltage relationships of normalized currents ($n = 12, 7$). Boltzmann parameters of the corresponding activation curves are given in the text. (C) Steady-state inactivation curves for 35-msec prepulses to the indicated potentials (holding potential -100 mV, test potential -15 mV, $n = 12, 7$). Continuous lines are fits to a single Boltzmann function; the dotted line represents the sum of two Boltzmann functions (parameters are given in the text).

Steady-state inactivation was determined measuring the peak current at -15 mV after 35-msec prepulses to the potentials indicated in Figure 2C; curves were fitted with the Boltzmann equation. The difference of 5 mV in $V_{0.5}$ between control (-93.7 ± 0.4 mV) and PC (-98.3 ± 3.1 mV) patches was not statistically significant ($p > 0.05$). However, there was a significant difference in the slope factor k_V (control: 8.4 ± 0.3 mV, $n = 12$, PC: 11.1 ± 0.3 mV, $n = 7$, $p < 0.001$, equivalent to the movement of 3.0 and 2.3 e_0 across the membrane), indicating a decreased voltage dependence for PC. Due to dominant inheritance, there should be two populations of sodium channels in PC muscle fibers: wild type (WT) and R1448P channels. Thus, the reduced slope should represent the sum of two Boltzmann functions. Attempts to fit the PC steady-state inactivation curve with free parameters of two Boltzmann functions failed. However, assuming a 50:50 contribution of WT and mutant channels in PC muscle and a -10 -mV shift and altered slope of

the inactivation curve of R1448P channels (values estimated from expressed R1448H/C mutations [9]), the following function yields a good superposition to the experimental data (Fig 2D, dotted line):

$$I/I_{\max} = 0.5/\{1 + \exp[(V + 93.7)/8.4]\} + 0.5/\{1 + \exp[(V + 104)/14]\}.$$

To illustrate the slower decay of PC Na^+ currents, representative control and PC currents are superimposed in Figure 3A. The time course of inactivation was analyzed by fitting the first 45 msec of the current decay to $I/I_{\max}(t) = g_1 \exp(-t/\tau_{h1}) + g_2 \exp(-t/\tau_{h2}) + C$, in which τ_{h1} and τ_{h2} are the time constants of inactivation and g_1 and g_2 , the relative amplitudes. The constant term, C , was generally smaller than 1.5% of the peak amplitude and therefore neglected (steady-state Na^+ currents were analyzed more accurately from single-channel recordings, see below). τ_{h1} was significantly

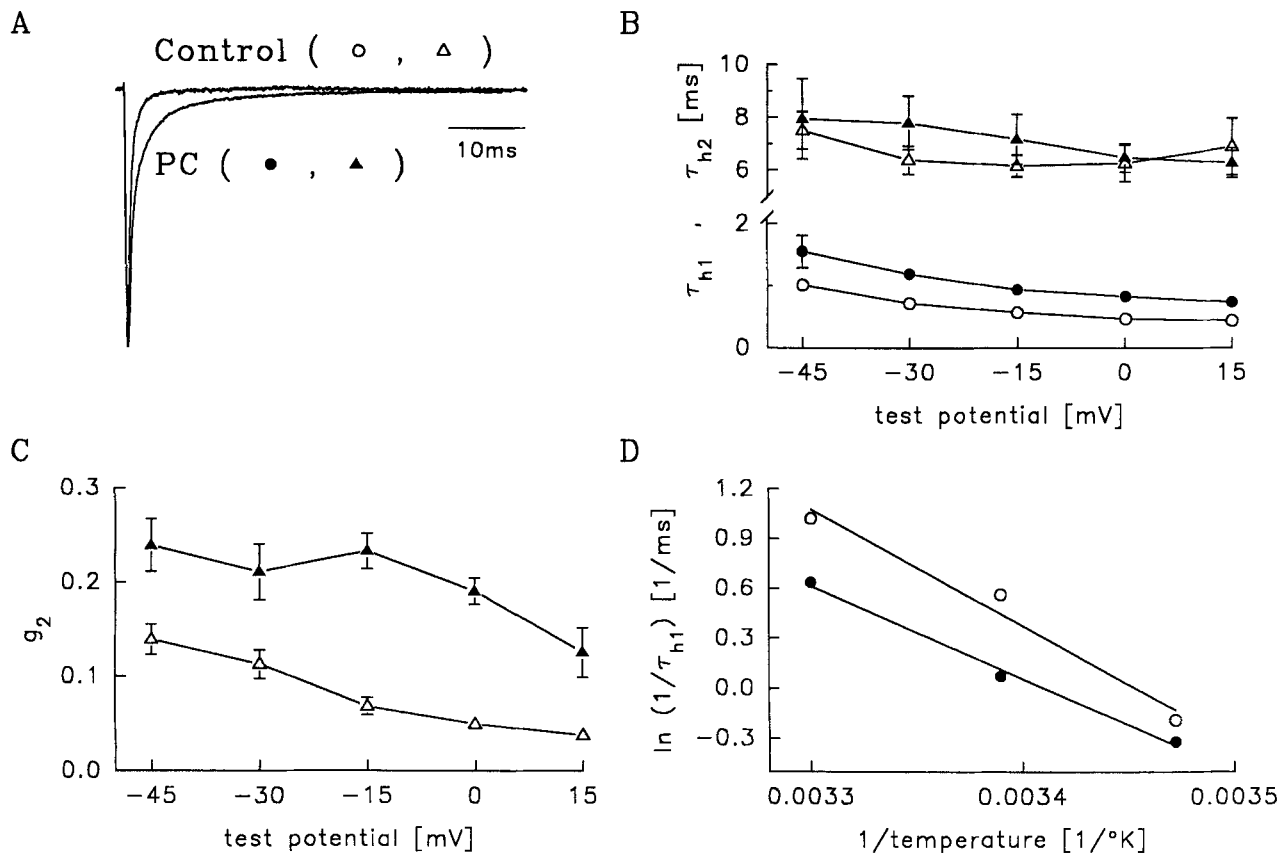


Fig 3. Time course of inactivation. (A) Superimposed normalized currents for paramyotonia congenita (PC) and control patches (test potential -15 mV). Symbols used in (B) through (D) are given in parentheses. The first 45 msec of the current decay was fitted to a second-order exponential. (B) Inactivation time constants, τ_{h1} (circles) and τ_{h2} (triangles) versus test potential; $n = 16, 7$. The differences between control and PC currents are statistically significant at all potentials ($p < 0.001$). (C) Relative amplitude, g_2 , of the slower exponential term versus test potential. There were statistically significant differences for all potentials ($p < 0.01$). (D) Arrhenius plots for mean values of τ_{h1} at 15, 22, and 30°C. The corresponding activation energies are given in the text.

increased for PC versus control currents ($p < 0.001$) and slightly less voltage dependent for PC (increase 1.5-fold at -45 mV and 1.8-fold at 0 mV, Fig 3B). Whereas τ_{h2} was similar for control and PC currents, g_2 was significantly increased for PC ($p < 0.01$, Fig 3C). Theoretically, there should be more than two time constants for PC because of the mixed-channel population. However, both control and PC data were equally well fitted to a third-order exponential without improving the fit compared to a second-order, and fitting to a fourth-order exponential failed. Thus, it is important to note that the double exponential only gives a quantitative description of the slowed inactivation for PC, without implying any model for sodium channel inactivation gating.

Since recovery from inactivation determines the refractory period after the action potential, a faster recovery can contribute to the genesis of myotonia as has been shown for all PC mutants [9, 12] and a PAM

mutant [10]. The time course of recovery from inactivation was measured at various "recovery potentials" in the range of -80 to -180 mV, using the pulse protocol indicated in Figure 4A. The time course of recovery was well fitted by a single exponential. Fitting the PC data by a double exponential failed. Recovery at -100 mV is shown in Figure 4A. In PC patches, the current did not reach the same level as for control patches, again illustrating the negative shift of the inactivation curve. At all investigated potentials, recovery time constants were slightly but not significantly increased for PC versus control patches (Fig 4B), in contrast to the faster recovery observed in other PC mutants measured in expression systems. We have no explanation for this unexpected result, but it should be mentioned that recovery for R1448H/C was only faster at -70 mV and was not different at -100 mV, compared to WT [9]. In the R1448P mutation occurring in native muscle, recovery from inactivation

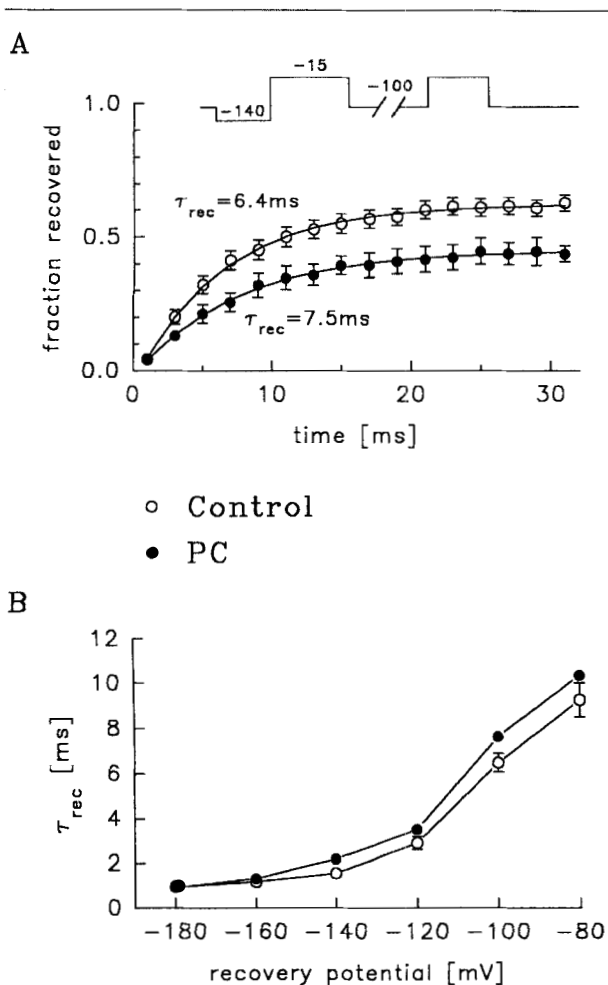


Fig 4. Recovery from inactivation. (A) Recovery at -100 mV: Patches were held at -100 mV and prepulsed for 35 msec to -140 mV in order to activate all Na^+ channels; subsequently, Na^+ channels were completely inactivated by a 50-msec pulse to -15 mV, and recovery was measured after pulses to the recovery potential (here -100 mV) using a second test pulse to -15 mV. Plotted is the ratio of the two pulses to -15 mV versus the time spent at the recovery potential. Lines are first-order exponential fits with time constants indicated; $n = 9, 5$. (B) Recovery time constant, τ_{rec} , versus recovery potential; $n = 3-9$.

does not appear to be important in the pathophysiology of myotonia and weakness.

SINGLE-CHANNEL STUDIES. The slowing of the current decay observed in macropatches can arise from (1) the later occurrence of first openings, (2) longer duration of openings, and (3) an increase in the number of reopenings, or a combination of these changes. For clarification, we examined Na^+ channel openings elicited by depolarizing steps from -100 to -30 mV (Fig 5A). Reopenings after the first short opening occurred either as single events (traces 3 of control, 2 and 3 of PC,

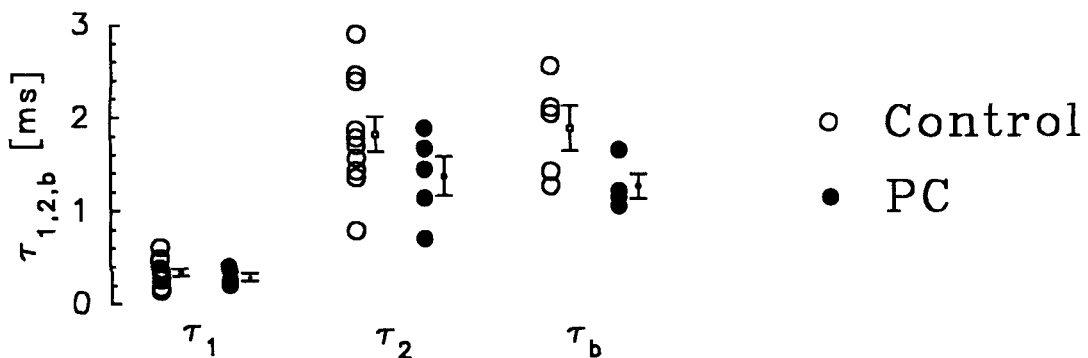
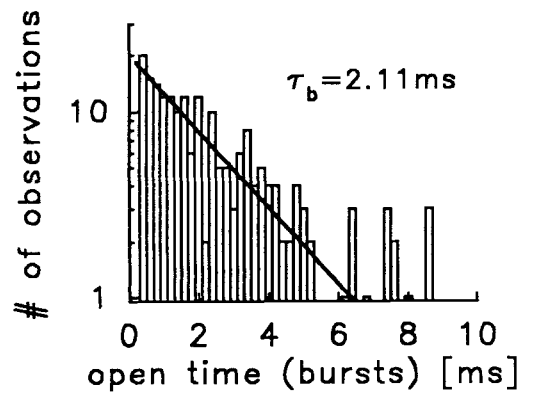
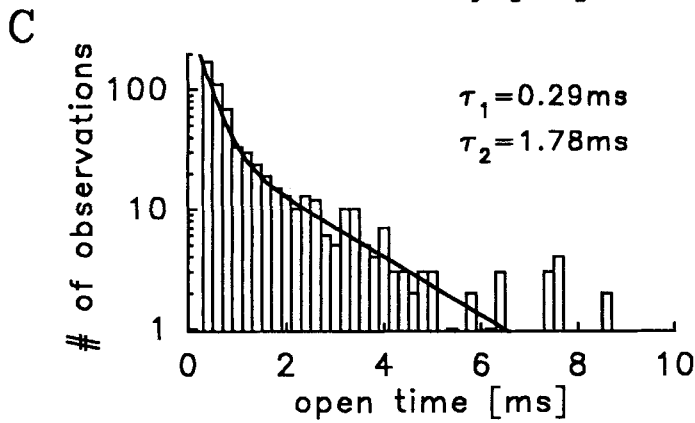
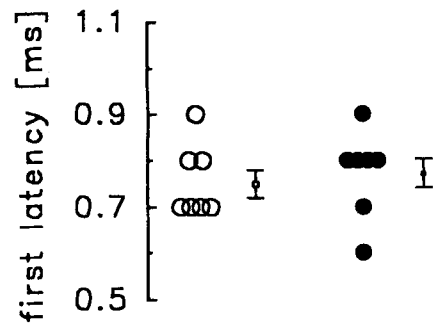
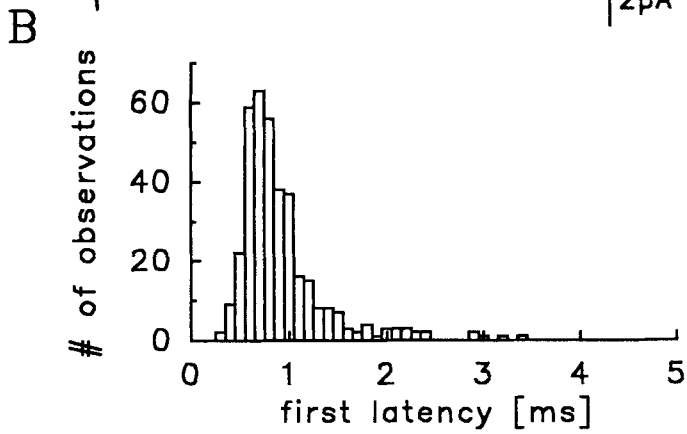
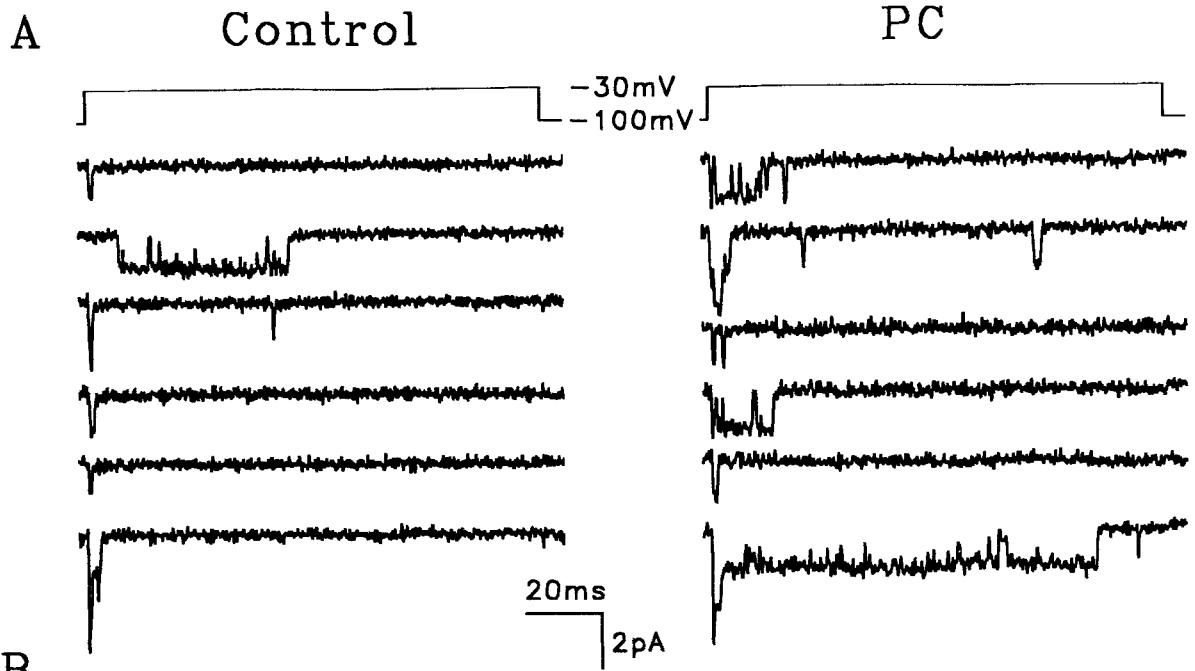
counted from top) or as bursts (traces 2 of control, 1 and 6 of PC). At least 300 traces per patch were recorded.

First latencies were evaluated from patches containing one to four channels. A first latency histogram derived from PC is shown in Figure 4B (left panel). To compare measurements from PC and control patches, cumulative latency distributions were corrected for the number of channels in the patch as described [23]. The corrected medians, shown in Figure 4B (right panel), were almost identical for control and PC patches (0.75 ± 0.07 msec vs 0.77 ± 0.09 msec).

Mean open time distributions were best fitted by the sum of two exponential functions using the method of maximum likelihood (see Fig 5C, upper left panel). To find out the origin of the slower time constant, τ_2 , channel bursts (e.g., traces 2 of control, 1 and 6 of PC, counted from top in Fig 5A) were evaluated separately. A burst was defined as repetitive openings lasting 10 msec or longer. Burst open time distributions were best fitted by a single exponential (see Fig 5C, upper right panel), yielding time constants, τ_b , similar to the slower time constant, τ_2 . Thus, we concluded that this second time constant derived from the occurrence of channel bursts. Significant differences between control and PC data were not seen for $\tau_{1,2}$ or for τ_b (see Fig 5C, lower panel). The relative amplitude of the second exponential component was also the same for control and PC patches ($42 \pm 5\%$ vs $43 \pm 3\%$).

Since first latencies and mean open times were unaltered in PC, we can conclude that the increased occurrence of reopenings contributed exclusively to the slowing of the current decay. The frequency of channel bursts was increased for PC versus control patches, but the relative occurrence of bursts in relation to all re-

Fig 5. Single-channel studies. (A) Current traces from a control and a paramyotonia congenita (PC) patch. Sodium channel openings, elicited by the indicated pulse protocol, are shown as downward deflections. Both patches contained four Na^+ channels. (B) Latencies to first openings. Left: Histogram of all first latencies to openings occurring in 500 depolarizations of a PC patch containing four Na^+ channels. Right: Arithmetic means of all first latencies occurring in each of seven control and seven PC patches and corresponding means \pm SEM, which are given in the text. (C) Mean open times. Upper left panel: Semilogarithmic histogram of open times of a control patch containing four channels; 1,000 depolarization steps were analyzed; the line represents a fit to a second-order exponential with time constants indicated. Upper right panel: Histogram derived from the same experiment for all openings occurring during bursts; the line is a first-order exponential fit. Lower panel: Values from all patches evaluated as shown in the upper two histograms. Means \pm SEM are as follows (control vs PC, in msec): τ_1 : $0.34 \pm 0.04, 0.29 \pm 0.04$; τ_2 : $1.82 \pm 0.19, 1.37 \pm 0.21$; τ_b : $1.88 \pm 0.24, 1.26 \pm 0.13$.



openings was the same for PC and control patches, indicating that there was no shift in gating modes.

As seen in Figure 3A, the macroscopic Na⁺ current declined to almost zero within about 40 msec. Assuming an average τ_{h2} of 8 msec and g_2 of 20% (see Figs 3B, 3C), the sodium current should have declined to 0.1% of its peak value after this period; that is, a steady state was reached (at 15°C, this value was 0.2%). To determine if there was an increased steady-state Na⁺ current in PC, the late current occurring between milliseconds 45 and 115 after onset of the depolarization was calculated for each trace and normalized to the average peak early current. Histograms, showing the steady-state current for each of 500 consecutive depolarizing pulses at 22°C, are presented in Figure 6A for a control and a PC patch, both containing four channels. High peaks represent bursts, whereas the lower peaks correspond to single late openings. Arithmetic means of I_{ss}/I_{peak} over all traces were significantly larger for PC patches (control: $0.5 \pm 0.1\%$, $n = 20$, PC: $1.2 \pm 0.1\%$, $n = 16$, 22°C, Fig 6B).

EFFECTS OF TEMPERATURE. The hallmark of PC is cold-induced stiffness and paralysis. Effects of temperature on the kinetics of Na⁺ channels were evaluated in the range of 15 to 30°C. Generally, a decrease in temperature resulted in slowing of the kinetics while an increase caused acceleration for both PC and control. However, inactivation was slower for PC than for control patches at any temperature. The values for activation energy, E_a , calculated from Arrhenius plots of mean values of τ_{h1} , were 48 and 56 J/mol for PC and control patches, respectively (see Fig 3D). Thus, the mutation had little influence on E_a and was even less temperature dependent than the control. τ_{h2} and g_2 did not show a different temperature dependence for control versus PC either.

The frequency of steady-state openings (I_{ss}/I_{peak} , see above) of mutant Na⁺ channels was increased at all temperatures, showing a maximum difference between PC and control at 15°C (see Fig 6B).

Discussion

Pathophysiology of Paramyotonia Congenita and Genotype-Phenotype Correlations to Other Sodium Channelopathies

A study of the functional consequences of the R1448P sodium channel mutation causing PC on native human skeletal muscle allowed us to correlate electrophysiological results at the cellular and single-channel level to clinical symptoms of the disease. The patient had a severe form of PC exhibiting paradoxical myotonia in a warm environment and cold-induced stiffness followed by weakness [14].

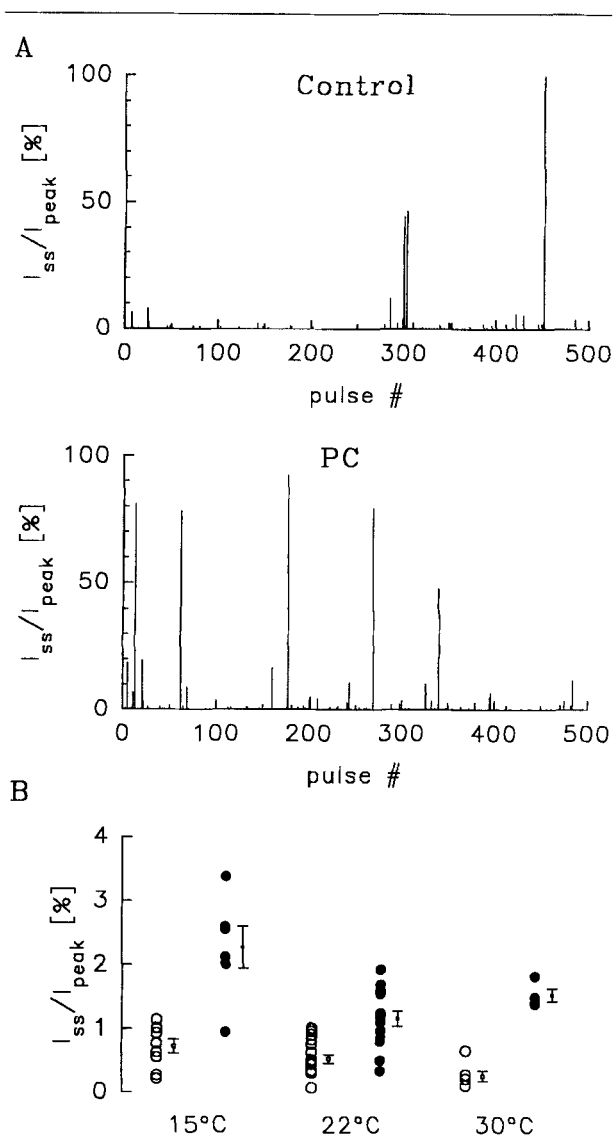


Fig 6. Late sodium channel openings. (A) Steady-state Na⁺ current, carried by openings occurring between milliseconds 45 and 115 of 500 consecutive test pulses to -30 mV, normalized to the average peak early current; both the control and the paramyotonia congenita (PC) patch contained four channels; temperature was 22°C. (B) Arithmetic means of I_{ss}/I_{peak} of 300 to 500 consecutive test pulses for all evaluated control and PC patches at 15, 22, and 30°C. Means \pm SEM are as follows (control vs PC, in %): 15°C: 0.73 ± 0.11 , 2.27 ± 0.33 ; 22°C: 0.53 ± 0.07 , 1.16 ± 0.12 ; 30°C: 0.26 ± 0.08 , 1.53 ± 0.10 . The differences between control and PC patches are statistically significant at all temperatures ($p < 0.001$).

PARADOXICAL MYOTONIA. The definition of paradoxical myotonia is muscle stiffness worsening with exercise in contrast to the “warm-up” phenomenon seen with chloride channel myotonia. It is a typical symptom of PC and only seldom seen in patients with other sodium channelopathies. Paradoxical myotonia is predominantly accompanied by a very slow current decay [9, 12], whereas myotonia (not aggravated by exercise) and paralysis are mainly accompanied by a more (HyperPP [7, 8]) or less (PAM [6, 10, 11]) increased steady-state current. A very slow current decay that prolongs action potentials may be a plausible explanation for paradoxical myotonia, since only continuous exercise would provide enough sodium influx to depolarize the muscle membrane and to induce spontaneous contractions.

COLD-INDUCED SYMPTOMS. The cold-induced weakness could be reproduced *in vitro* and was shown to occur when a certain threshold of depolarization was exceeded. Since the depolarization only occurred with muscle cooling and in the absence of TTX, it was clearly induced by sodium channel activity. In agreement, the increase in late sodium channel openings was maximal for PC at the lowest temperature (15°C). A small steady-state sodium current could produce myotonia, whereas paralysis would occur when the persistent sodium conductance exceeds a certain amount, that is, becomes so large that most sodium channels will be inactivated due to depolarization. This is supported by a computer model [24], and experimental results on HyperPP and PAM. For expressed sodium channels causing HyperPP, the I_{ss}/I_{peak} was 6 to 8% [7], whereas for those causing PAM it was only 3% [10, 11]. Resting membrane potentials in HyperPP were decreased to -40 mV and muscle fibers were inexcitable [2], whereas in PAM, fibers were still excitable and resting potentials only decreased to -60 mV [6]. In this study and in earlier studies on PC [3,16], resting membrane potentials decreased to -40 mV only with cooling.

The question arises as to why the most obvious parameter altered in PC, the current decay, was less temperature dependent than that in controls. Since there are two populations of sodium channels in PC muscle, R1448P and WT (dominant inheritance), R1448P channels might have been inactivated to a greater extent at 15°C than at higher temperatures. This would decrease the percentage of available mutated channels and thus conceal the difference in the time course of inactivation between PC and control fibers. However, since R1448P channels inactivate incompletely (i.e., reopen), the steady-state sodium current was increased at 15°C. If this hypothesis is valid, the left shift of the inactivation curve of R1448P channels would have to be temperature dependent and could also contribute to muscle weakness by decreasing the number of sodium channels that can be activated. In agreement with this

hypothesis, a left-shifted inactivation curve is only seen for sodium channel mutations causing PC with weakness (R1448H/C/P [9, 12]). In contrast, the inactivation curve is shifted to the right for L1433R causing PC without weakness [12, 25]. A similar shift to the right was observed for various mutations causing PAM [10, 11], characterized by the absence of weakness. Hence, a right-shifted inactivation curve could in turn prevent weakness in the latter diseases.

In conclusion, we propose that stiffness and weakness with cooling in PC are induced by the combination of an increased steady-state sodium current and a left-shifted inactivation curve. In a cold environment, mutant sodium channels more easily enter the inactivated state from which they reopen, thereby depolarizing the muscle fiber and inactivating additional (mutant and later normal) channels.

Single-Channel Results and Consequences of the R1448P Mutation for Sodium Channel Gating

The slowing of the decay of the macroscopic sodium current was shown to be exclusively the result of an increased frequency of channel reopenings, since mean open times and first latencies were not altered compared to controls. A thorough analysis of these reopenings revealed two modes of gating: short single events and longer repetitive openings, so-called bursts [26]. These two gating modes exhibited different mean open times, suggesting a second open state for bursts. Patlak and Ortiz [26] proposed that bursts occur due to an occasional switch of the inactivation gate to a nonfunctional mode. It is important to note that both control and PC fibers exhibited modal gating and that there was no shift in gating modes for PC toward a more frequent occurrence of bursts. Instead, both single events and bursts of late openings occurred more frequently in PC fibers. This supports the hypothesis of Chahine and colleagues [9] providing the same kinetic scheme for both control and PC, with altered rate constants for PC. However, in contrast to our study, Chahine and colleagues used short depolarizing test pulses (15 msec) and did not find evidence for modal gating.

Our data are consistent with the conclusion that segment S4 of the fourth repeat (IV) may be more important for channel inactivation than for activation [9]. R1448 mutations may impair outward movement of the IVS4 segment so that binding of the inactivation gate is delayed, resulting in a slowed current decay. In contrast, mutations within the inactivation gate (G1306E/V/A [6, 11]) or its possible docking site (V1589M [10], M1592V [7]) may reduce binding affinity, producing a larger steady-state current and only a slight increase in τ_h .

This study was supported by the Deutsche Forschungsgemeinschaft (Le481/3-2), the Muscular Dystrophy Association, and the Deutsche Gesellschaft für Muskelkranke (Le 1/95).

We thank Dr K. Ricker for reexamining the patient, Dr D. Pongratz for performing the histology, Dr S. Quasthoff for providing the K⁺ channel opener, Dr R. Rüdél for helpful comments on the manuscript, Ms M. Rich for language editing, Ms U. Mohr for technical assistance, and Ms S. Plate for secretarial help.

References

1. Hoffman EP, Lehmann-Horn F, Rüdél R. Over-excited or inactive: ion channels in muscle diseases. *Cell* 1995;80:681–686
2. Lehmann-Horn F, Küther G, Ricker K, et al. Adynamia episodica hereditaria with myotonia: a non-inactivating Na⁺ current and the effect of extracellular pH. *Muscle Nerve* 1987;10:363–374
3. Lehmann-Horn F, Rüdél R, Ricker R. Membrane defects in paramyotonia congenita (Eulenburg). *Muscle Nerve* 1987;10:633–641
4. Cannon SC, Brown RH, Corey DP. A Na⁺ channel defect in hyperkalemic periodic paralysis: K⁺ induced failure of inactivation. *Neuron* 1991;6:619–626
5. Lehmann-Horn F, Iaizzo PA, Hatt H, Franke C. Altered gating and conductance of Na⁺ channels in hyperkalemic periodic paralysis. *Pflügers Arch* 1991;418:297–299
6. Lerche H, Heine R, Pika U, et al. Human Na⁺ channel myotonia: slowed channel inactivation due to substitutions for a glycine within the III-IV linker. *J Physiol* 1993;470:13–22
7. Cannon SC, Strittmatter SM. Functional expression of Na⁺ channel mutations identified in families with periodic paralysis. *Neuron* 1993;10:317–326
8. Cummins TR, Zhou J, Sigworth FJ, et al. Functional consequences of a Na⁺ channel mutation causing hyperkalemic periodic paralysis. *Neuron* 1993;10:667–678
9. Chahine M, George AL Jr, Zhou M, et al. Na⁺ channel mutations in paramyotonia congenita uncouple inactivation from activation. *Neuron* 1994;12:281–294
10. Mitrovic N, George AL Jr, Heine R, et al. K⁺-aggravated myotonia: destabilization of the inactivated state of the human muscle Na⁺ channel by the V1589M mutation. *J Physiol* 1994;478:395–402
11. Mitrovic N, George AL Jr, Lerche H, et al. Different effects on gating of three myotonia-causing mutations in the inactivation gate of the human muscle sodium channel. *J Physiol* 1995;487:107–114
12. Yang N, Ji S, Zhou M, et al. Sodium channel mutations in paramyotonia congenita exhibit similar biophysical phenotypes in vitro. *Proc Natl Acad Sci USA* 1994;91:12785–12789
13. Isom LL, De Jongh KS, Patton DE, et al. Primary structure and functional expression of the β_1 subunit of the rat brain Na⁺ channel. *Science* 1991;256:839–842
14. Wang J, Dubowitz V, Lehmann-Horn F, et al. In vivo structure/function studies: consecutive Arg1448 changes to Cys, His, and Pro at the extracellular surface of IVS4. In: Dawson DC, Frizzell RA, eds. *Ion channels and genetic diseases*. New York: Rockefeller University Press, 1995:77–88
15. Lehmann-Horn F, Iaizzo PA. Resealed fiber segments for the study of the pathophysiology of human skeletal muscle. *Muscle Nerve* 1990;13:222–231
16. Lehmann-Horn F, Rüdél R, Dengler R, et al. Membrane defects in paramyotonia congenita with and without myotonia in a warm environment. *Muscle Nerve* 1981;4:396–406
17. Hamill OP, Marty A, Neher E, et al. Improved patch-clamp techniques for high-resolution current recording from cells and cell-free membrane patches. *Pflügers Arch* 1981;391:85–100
18. Quasthoff S, Franke C, Hatt H, Richter-Turtur M. Two different types of potassium channels in human skeletal muscle activated by potassium channel openers. *Neurosci Lett* 1990;119:191–194
19. Lerche H, Fahlke Ch, Iaizzo PA, Lehmann-Horn F. Characterization of the high-conductance Ca²⁺-activated K⁺ channel in adult human skeletal muscle. *Pflügers Arch* 1995;429:738–747
20. Horn R. Estimating the number of channels in patch recordings. *Biophys J* 1991;60:433–439
21. Grafe P, Quasthoff S, Strupp M, Lehmann-Horn F. Enhancement of K⁺ conductance improves in vitro the contraction force of skeletal muscle in hypokalemic periodic paralysis. *Muscle Nerve* 1990;13:451–457
22. Quasthoff S, Spuler A, Spittelmeister W, et al. K⁺ channel openers suppress myotonic activity of human skeletal muscle in vitro. *Eur J Pharmacol* 1990;186:125–128
23. Parlak J, Horn R. Effects of N-bromacetamide on single channel currents in excised membrane patches. *J Gen Physiol* 1982;79:333–351
24. Cannon SC, Brown RH, Corey DP. Theoretical reconstruction of myotonia and paralysis caused by incomplete inactivation of sodium channels. *Biophys J* 1993;65:270–288
25. Ptáček LJ, Gouw L, Kwiecinski H, et al. Sodium channel mutations in paramyotonia congenita and hyperkalemic periodic paralysis. *Ann Neurol* 1993;19:300–307
26. Parlak J, Ortiz M. Two modes of gating during late Na⁺ channel currents in frog sartorius muscle. *J Gen Physiol* 1986;87:305–326